Original article

Genetic diversity and biological activity of *Curcuma longa* ecotypes from Rapa Nui using molecular markers

Cristóbal Balada [a], Mónica Castro [b], Claudia Fassio [b], Agustín Zamora [a], María José Marchant [a,b], Waldo Acevedo [a], Leda Guzmán [a,*]

[a] *Laboratorio de Química Biológica, Instituto de Química, Facultad de Ciencias, Pontificia Universidad Católica de Valparaíso, Valparaíso, Chile*
[b] *Laboratorio de Propagación, Escuela de Agronomía, Pontificia Universidad Católica de Valparaíso, Quillota, Chile*

A B S T R A C T

Curcuma Longa (*CL*) has been used for hundreds of years by native people from Rapa Nui for the treatment of different illness. Despite this plant was introduced from Polynesia or India, there is still scarce information about its origin. The objective of this study was to analyze the genetic variation of three *CL* ecotypes based on molecular phylogenetic and genotypification using internal transcribed spacer 2 (ITS2) and simple sequence repeats (SSR). Antioxidant and anti-inflammatory properties of rhizomes and leaves extracts of three *CL* plants were analyzed by spectrophotometric methods and cyclooxygenase 2 (COX-2) inhibition assay. Complementarily, we predicted the potential binding mode and binding energy of curcuminoids and nonsteroidals anti-inflammatory drugs (NSAIDs) into COX-2 via molecular docking. The ITS2 sequence shows two major clusters (I and II), group I consisted of *Curcuma haritha* and group II consisted of different species of Curcuma and Rapa Nui samples (MR-1, MR-2 and RK-2). Results of SSR markers show that genotype MR-2 was similar to MR-1 and RK-2 with 70.8 and 42.9% similarity, whereas genotype was similar to RK-2, MR-1 and MR-2 with 63.9, 43.2 and 42.9% similarity, respectively. MR-1 have better antioxidant and autoinflammatory activity than rest of *CL* samples due to its high concentration of polyphenols (33.68 mg/g) and curcumin (29.69 mg/g). Furthermore, docking results show that three curcuminoids of *CL* and selective NAIDs, as celecoxib, etodolac and meloxicam, share the same binding pocket into COX-2. However, three curcuminoids have a lower $\Delta G_{binding}$ than other COX-2 selective NAIDs as etodolac and meloxicam, except for Coxib family as valdecoxib, celecoxib and rofecoxib. Our findings suggest MR-1, MR-2 and MK-2 from Germplasm Bank (Mataveri Otai of CONAF) are closely related to *Curcuma amada* and *Curcuma montana* even though they have genetic variability.

© 2020 The Authors. Published by Elsevier B.V. on behalf of King Saud University. This is an open access article under the CC BY-NC-ND license (http://creativecommons.org/licenses/by-nc-nd/4.0/).

1. Introduction

The genus Curcuma, belonging to the family Zingiberaceae, includes approximately 100 species around the world and widely used in the traditional medicine in China and India (Sigrist et al., 2010). The rhizome of *Curcuma longa* (*CL*) is widely used as integral ingredient of Indian cooking, medicinal drug and to a lesser extent as cosmetic and food preservatives (Prasad and Aggarwal, 2011; Xiang et al., 2011). Among the compounds found in *CL* are essentials oils, minerals, polyphenolic and terpenoid compounds (Duvoix et al., 2005; Hatcher et al., 2008). Among these polyphenolic compounds, curcumin (1,7-bis-(4-hydroxy-3-methoxyphenyl)-1,6-heptadiene-3,5-dione) is the most important compound because of its therapeutic or pharmacological properties. Indeed, anti-inflammatory, antifungal and antitumoral activities are principally attributed to the content of curcumin and its analogs (Fig. 1) (Siju et al., 2010; Strimpakos and Sharma, 2008; Tomeh et al., 2019). Other species of curcuma are also widely used for medicine and culinary use as *C. aromatica*, *C. amada C. kwangsiensis*, *C. ochrorhiza*, *C. pierreana C. zedoaria*, *C. malabarica*, among others (Sasikumar, 2005).

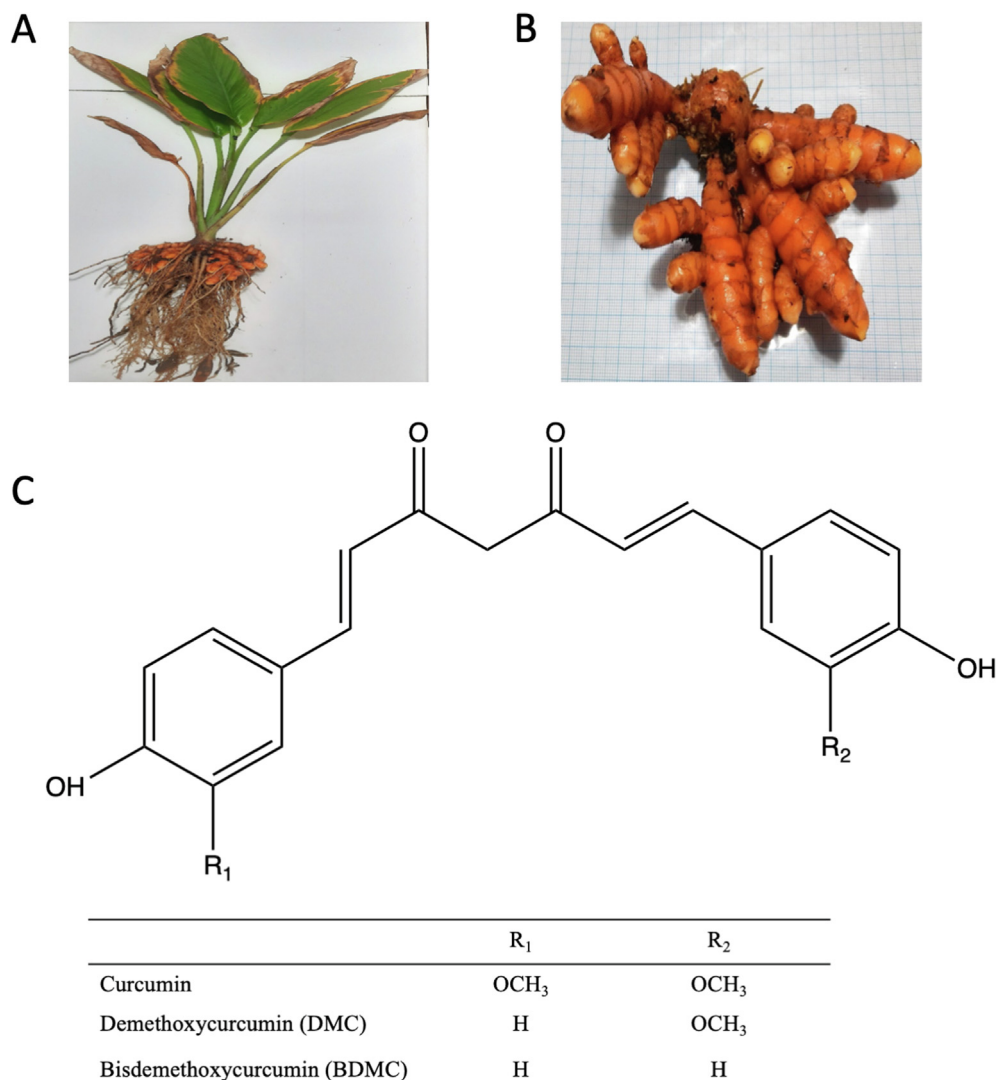*CL* is also found in Chile, specifically in Rapa Nui Island, where is considered a magical plant for the native people, being used for

	R₁	R₂
Curcumin	OCH₃	OCH₃
Demethoxycurcumin (DMC)	H	OCH₃
Bisdemethoxycurcumin (BDMC)	H	H
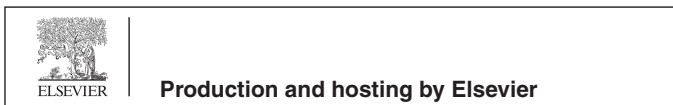
Fig. 1. Illustrative of (A) leaves and (B) rhizome of *Curcuma longa* (C) Chemical structure of the major curcuminoids from *Curcuma longa* extracts.

treatment of several diseases as cancer, diabetes, muscle pain and other illness (Kocaadam and Şanlier, 2017). Studies, reported between 1891 and 2005, suggest that *CL* is a plant introduced from Polynesia and probably native from India (Dubios et al., 2013). Nonetheless, until now its origin is unknown, and its massive use compromises the preservation of this species. Furthermore, some studies have reported that exist a difference in the content of curcumin and others active molecules among individuals of *CL*. This difference of chemical profile could be due to genetic variety and distribution geographic (Arya et al., 2016; Hayakawa et al., 2011). For this reason, it is necessary to use molecular markers to an appropriate characterization of *CL* found in Rapa Nui. DNA barcoding is a molecular diagnostic technique that allows the identification of species using a short a standardized DNA region (Arif et al., 2011). The ITS2 is part of the eukaryotic nuclear rDNA (between the 5.8S and the 28S rRNA) and allows to carry out phylogenetic analyses and classification at the species level using highly conserved priming sites to DNA amplification (Feng et al., 2016; Arif et al., 2011). In addition, genomic microsatellite markers, as the use of simple sequence repeat markers (SSR), has been utilized for a specific genotyping in a wide variety of plants (Siju et al., 2010; Sigrist et al., 2011; Tóth et al., 2000).

The objective of this study was to analyze the genetic variation of three *CL* ecotypes, from Mataveri Otai reservoir in Hanga Roa, based on molecular phylogenetic and genotypification using internal transcribed spacer 2 (ITS2) and simple sequence repeats (SSR). Furthermore, we evaluated the impact of the genetic variation on the content of active metabolites as curcumins, phenolic and tannins (Siju et al., 2010). Furthermore, we investigated the antioxidant properties in rhizomes and leaves to analyze the relationship between the metabolite contents and the genetic variability of three *CL* plants found in Rapa Nui. Additionally, we analysis the anti-inflammatory properties of extracts from *CL* plants through cyclooxygenase-2 (COX-2) inhibition activity assay and we predicted the potential binding mode and binding energy of curcuminoids and traditional nonsteroidals anti-inflammatory drugs (NSAIDs) into COX-2 via molecular docking. The anti-inflammatory mechanism on COX-2 may contribute in medicinal actions of *CL* plants - as anticarcinogenic - for being used for treatment of different types of cancer as colon, breast cancer, and other tumors that overexpress COX-2 (Xu et al., 2014). Finally, polymorphic and genetic variability information and its relationship with the biological activity of studied three *CL* plants could be relevant for an adequate culture and propagation of this vulnerable specie in Rapa Nui.

2. Materials and methods

2.1. Chemicals and plant material

2.1.1. Chemicals

Gallic acid, 2,2-diphenyl-1-picrylhydrazyl radical (DPPH), AAPH, TROLOX, ethanol and n-hexane were purchased from Sigma-Aldrich (St. Louis, MO, USA). Curcumin, Folin-Ciocalteu reagent, sodium carbonate and methanol (MeOH) were purchased from Merck Co.

2.1.2. Plant material

Three *CL* plants were obtained from the Germplasm Bank of Mataveri Otai of CONAF in Rapa Nui (geographic coordinates: 27°09′50, 17′S-109°26′24,63O). These *CL* plants were named as MR-1, MR-2 and RK-2 and used in this investigation. Furthermore, a rhizome sample of *CL* from Peru (Continental Curcuma or CC) was used as a control to validate the results of SSR markers. The collected samples were packed into sterile polybags and its transportation was carried out to 4 °C.

2.2. Genetic diversity analysis

2.2.1. Genomic DNA extraction

Leaves and rhizomes from MR-1, MR-2, RK-2 and CC were cleaned, washed with free nuclease water. The DNA extraction of samples was performed using the NucleoSpin® Plant II kit (Machery-Nagel, Düren, Germany), according to manufacturer's instructions. The DNA integrity was analyzed using 0.8% agarose gel, stained with ethidium bromide, the quantity and quality of the DNA was evaluate measurement the absorbance to 260 nm and the ratio 260/280 nm using EPOCH microplate reader (BioTek® Instruments).

2.2.2. Genetic identification of different CL samples

The nrDNA ITS2 region were analyzed by PCR amplification. The sequencing of PCR products (Seoul, South Korea; www.macrogen.com) were used to identify the species of *CL* from Rapa Nui. ITS2 sequences were retrieved from GenBank to identify homologous sequences using BLAST search. The ITS2 primers (Forward: ATGC-GATACTTGCTGTGAAT and Reverse: GACGCTTCTCCAGACTACAAT) were used to identify *CL* samples as described by Chen et al. (2010). The PCR reaction was performed in a 20 μL reaction system containing 2.5 mM MgCl$_2$, 0.2 mM dNTP's, 0.25 μM of each primer, 50 ng of genomic DNA and 0.5 μL of enzyme (1U/μL, KAPA HiFi HotStart, Biosystems). PCR reactions were performed on a T100TM Thermal Cycler (BioRad, Hercules, CA, USA) using the following temperature cycling parameters: initial denaturation for 3 min at 95 °C followed by 35 cycles of denaturation at 98 °C for 40 sec, annealing temperature at 52 °C for 20 sec and extension at 72 °C for 20 sec, and a final extension step at 72 °C for 5 min. PCR product were separated using 2% agarose gel stained with ethidium bromide and the size of the amplifications was estimated using 50 bp DNA Ladder (New England, BioLabs). To construct a phylogenetic tree based on the ITS sequences of different Curcuma species, the amplified regions were aligned using ClustalW (Thompson et al., 1994). Phylogenetic relationships were analyzed using the neighbor-joining (NJ) method using the JALVIEW program (Waterhouse et al., 2009).

2.2.3. Analysis of SSR marker and interpretation of sequence of CL plants

The polymorphisms and genetic relationships of three *CL* plants were evaluated using a set of eight SSR markers to *CL* designed as Curcuma microsatellite (CuMiSat) (Siju et al., 2010) showed in the

Table 1. The PCR reaction was performed as indicated above and the PCR products were analyzed using 3% agarose electrophoresis (UltraPure™ Agarose-1000) and stained with ethidium bromide. Pictures of the pattern of bands were taken and stored as digital images to be analyzed (Figure S1). Reproducible data (number of PCR fragment, sharp bands) were used to estimate the genetic similarity between *CL* accessions. Data were annotated as presence (1) and absence (0) of bands. A total of 37 microsatellites (PCR fragment) were selected in order to analyze the genetic variability between three *CL* plants and CC. Dendrogram was generated using the UPGMA sequential clustering method through the DendroUPGMA web server (URL: genomes.urv.cat/UPGMA) (Garcia-Vallve et al., 1999), whose data were recorded in a binary matrix, as individual accessions, using the Jaccard coefficient to compare the set of variables (Chattopadhyay, 2017; Siju et al., 2010).

2.3. Determination of metabolite composition and antioxidant activity of extract from CL plants

2.3.1. Extract preparation

Total phenolic compounds as polyphenols, tannins and curcumin were determined in samples from leaves and rhizomes of MR-1, MR-2, RK-2 and CC (as control). The samples from leaves and rhizomes were cleaned, washed with deionized water, and dried at 40 °C for two weeks (*see Supplementary Table ST1*). After drying, the rhizomes and leaves samples were ground to a powder (20 g approximately) and the lipids were subsequently extracted by Soxhlet with n-hexane as described by (Efthymiopoulos et al., 2019). Then, the extract solid from rhizome and leaves were re-extracted with 90% ethanol. Briefly, 90% ethanolic extract was prepared by adding extracts solids (MR1-Leaves: 2,129 g; MR-1-Rhizome: 1,789 g; MR-2 Leaves: 1,240 g; MR-2 Rhizome: 1,355 g; RK-2 Leaves: 1,741 g; RK-2 Rhizome: 1,115 g; CC: 2,784 g), the solutions were placed in the dark to avoid oxidation of ethanolic extracts and were shaken in a shaker for 72 h at 37 °C. Then, the solutions were filtered through Whatman No. 1 filter paper. Then, these extracts were dried and concentrated using a rotary evaporator (Heidolph, Germany) under reduced pressure (100 psi) at 40 °C. Finally, the extracts were resuspended in DMSO at 1 mg/mL as stock solution and preserved at −20 °C until use.

2.3.2. Determination of total phenolic compounds

Folin-Ciocalteu reagent was used to quantify the total polyphenol content in leaves and rhizomes. To this end, ethanolic extract was prepared from leaves and rhizomes as described by Ricco et al. (2015). Briefly, 100 μL of the samples of extracts from leaves and rhizomes (MR-1, MR-2, RK-2) were diluted 1:10 with water and 125 μL of Folin-Ciocalteu 1 N reagent, then were shaken vigorously. Then, 625 μL of 20% Na$_2$CO$_3$ was added and samples again were shaken for two hours. Finally, the absorbance was measured at 760 nm in a HPUV 8453 (Agilent, USA) spectrophotometer. The absorbance values were interpolated using a Gallic acid standard curve (0–10 mg/L) and the total phenolic content was expressed as mg of Gallic acid equivalents (GAE) per gram of dried extract. The experiment was performed in triplicate.

2.3.3. Determination of tannins

A modified Folin-Ciocalteu method was used for the quantification of tannins (Ricco et al., 2015). Briefly, 100 μL of extracts from leaves and rhizome (MR-1, MR-2, RK-2) and 500 μL of water were mixed with 250 μL of Folin-Ciocalteu 1 N reagent under vigorous shaken. Then, 35% Na$_2$CO$_3$ was added and the sample again was shaken for 30 min. The absorbance was measured at 725 nm and data were interpolated on a calibration curve of gallic acid. The

Table 1
Primer sequence used in SSR to analyze *Curcuma longa* ecotypes from Rapa Nui.

SSR Name	Sequence Forward	Sequence Reverse	T_a (°C)
CURS	GAGAAGGCCATCAAGGAGTGGG	GTTGTTCTCGGCGAGGTCCTTGGC	57
CuMiSat-01	AAACCGCAAGAAAACTGAAG	CTCTTCCCTGAACGATTCC	47
CuMiSat-02	TATGTGATGGTTGGGACG	GTAGTGGAGGAAGACGCC	48
CuMiSat-03	GCACTACTTCCTTCTCGTTCAA	CGTCGTAAAGATTAGCGTGTG	50
CuMiSat-04	TCAGGTTTCAGGGTGTAGAAG	CCCAGCAAGATTTTACCAAG	48
CuMiSat-05	AGCAGTGCGTCTTTCATC	CTCTTGTCACGGAACCTC	48
CuMiSat-06	AAGAAACTCCAACCACAATCC	CTTGTCTTCCTCCTCCATTG	48
CuMiSat-07	AGCATGTGTCTAGCTCTTTGC	AAGCAGTCGTTCCTCTACTGAC	51
CuMiSat-08	CATTGCGTGCCCACTTCC	CCTCCCTGTCGCTCTCCTC	53

results are expressed as mg of GAE per g of dried extract as indicated above. These experiments were performed in triplicate.

2.3.4. Determination of curcumin

The amount on curcumin in leaves and rhizomes (MR-1, MR-2, RK-2) were analyzed using a curcumin standard calibration curve (1 to 25 μg/mL), according to the modified protocol by Hazra et al. (2015). These experiments were performed in triplicate.

2.4. Antioxidant capacity

2.4.1. Antioxidant capacity by DPPH assay

The antioxidant activity of the extracts was evaluated by the DPPH (1,1-diphenyl-2-picrylhydrazyl) assay (Brand-Williams et al., 1995). Briefly, 1 mL of DPPH radical solution 0.1 mM in ethanol was mixed with 50 μL of the extract of leaves and rhizomes in various concentrations (50–800 μg/ml in ethanol). DPPH is reduced by antioxidant compound causing colour changes from purple to yellow. Colour change was measured [Absorbance (Abs)] at 518 nm after 20 min of reaction using an Epoch ELISA reader (ELx800, BioTek, VT, USA). The percentage of DPPH inhibition was calculated using the following equation:

$$\% \text{radicals scavenging activity} = \left(\frac{Abs control - Abs sample}{Abs control} \right) \times 100$$

where *Abs control* is the absorbance of DPPH in the absence of a sample and *Abs sample* is the absorbance of DPPH in the presence of a sample or the standard (gallic acid). The radical scavenger activity was expressed in terms of concentration of antioxidants necessary to scavenge 50% of DPPH free radical (IC_{50}). The IC_{50} value for each sample was determined graphically by plotting the percentage disappearance of DPPH as a function of the sample concentration. These experiments were performed in triplicate.

2.4.2. Antioxidant capacity by ORAC-FL assay

The ORAC value was measured according method described by Ou et al. (2001) with modifications from (Dávalos et al., 2004). The reaction was carried out in sodium phosphate buffer (75 mM, pH 7.4) using black-walled 96-well plates in a final volume of 200 μl. 20 μL of each extract and fluorescein (120 μL; 70 nM, final concentration) solutions were placed in each well of microplate. The mixture was preincubated for 15 min at 37° C. AAPH solution (60 μL; 12 mM final concentration) and quickly added. Later the microplate was immediately read using a fluorescence reader (Synergy HT multi-detection microplate reader; Bio-Tek Instruments, Inc., Winooski, VT, USA). The fluorescence was recorded for 80 min. The area under the fluorescence decay curve (AUC) was calculated as:

$$AUC = 1 + \sum_{i=1}^{i=80} \frac{f_i}{f_0}$$

where f_0 is the initial fluorescence reading at 0 min and f_i is the fluorescence reading at time i. The AUC corresponding to a sample is

calculated by subtracting the AUC corresponding to the blank space. Regression equations between net AUC and antioxidant concentration are calculated for all samples. ORAC-FL values are expressed as Trolox equivalents using the standard curve calculated for each assay. Results were expressed in μmol of Trolox equivalent/μmol of extract. These experiments were performed in triplicate.

2.4.3. COX-2 inhibitor screening

Assessment of cyclooxygenase-2 (COX-2) enzyme inhibition was carried out by using the BioVision® "COX-2 Inhibitor Detection Kit (Fluorometric)" kit. Briefly, the bioconversion of arachidonic acid to inflammatory prostaglandins (PGs) is not carried out as consequence of the inhibition of enzyme COX-2. Measurements were made over time, incubating MS extracts (3 μg/mL) and celecoxib (3 μg/mL) (as control of inhibition) measuring fluorescence (Ex/Em = 535/587 nm) in a multiplate reader (Thermo Scientific Skanit® Appliskan) at 25° C for 10 min. The inhibition % was calculated from the following formula:

$$\% Relative Inhibition = \frac{Slope of EC - Slope of S}{Slope of EC} X 100$$

2.5. Computational details

2.5.1. Molecular docking of ligand-protein interaction

We evaluate the interaction between COX-2 and curcuminoid polyphenols found in *CL*, as curcumin, demethoxycurcumin and bisdemethoxycurcumin, via molecular docking. To this end, the crystal structure of COX-2 (PDB code 3LN1) was retrieved from the Protein Data Bank (Berman et al., 2000), whereas the 3D structure of curcumin, demethoxycurcumin and bisdemethoxycurcumin, etodolac, rofecoxib, valdecoxib, lumiracoxib, celecoxib, etoricoxib and meloxicam were retrieved in SDF file format from the PubChem database at NCBI (Pubchem CID: 969516, 5469424, 5315472, 3308, 5090, 11960, 151166, 2662, 123619, 54677470, respectively). Etodolac, rofecoxib, valdecoxib, celecoxib, etoricoxib, meloxicam and nabumetone were used as reference compounds to compare their affinity to COX-2 with that of curcuminoid polyphenols because they are COX-2 selective non-steroidal anti-inflammatory drugs (NSAIDs) (Chen et al., 2008). Here we performed rigid docking taking whole receptor in order to identify the potential binding site and associated binding energy. Both ligands and protein were prepared using AutoDock Tools version 1.5.6 (ADT), as previously described (Guzmán et al., 2020). Finally, graphic analysis of molecular docking studies were performed using VMD (Humphrey et al., 1996).

2.6. Statistical analysis

The one-way analysis of variance followed by Tukey's post-test was used for comparisons. A $p < 0.0001$ was considered as statistically significant difference. All the statistical analyses were calculate using the computer software GraphPad Prism 8 (GraphPad

Software, San Diego, CA, USA). The concentrations of total polyphenols, curcumin and tannins were expressed as percentage in the extract (mg/g).

3. Results

3.1. Phylogenetic analysis based on ITS2 sequences

In this study, the nrDNA ITS2 region was used to identify species, using phylogenetic analyses, of three *CL* plants collected from Germplasm Bank of Mataveri Otai localized within Rapa Nui. The size of the ITS2 sequences used in the analyses ranged from 214 to 272 bp, with an average of 243 bp. The ITS2 sequences of 15 species of Curcuma (i.e. *longa, amada, haritha, montana, ferruginea, aromatica, caesia, amarissima, phaeocaulis, yunnanensis, kwangsiensis, aeruginosa, aff. Prakasha, zedoaria* and *flaviflora*) were retrieved from GenBank (Table 2). Results indicated that all the analyzed samples of CL have a 100% of sequence identity against *Curcuma longa voucher* pH *12,847* and *Curcuma amada*, followed by *Curcuma haritha, Curcuma montana* and *Curcuma ferruginea*, with a sequence identity of 98.74, 98.34 and 96.71%, respectively. The evolutionary relationships of the taxa *Curcuma* were inferred using the Neighbor Joining clustering method (Fig. 2). The phylogenetic tree shows two major clusters (I and II), group I consisted of *Curcuma haritha* and group II consisted of different species of Curcuma, CC and Rapa Nui samples (MR-1, MR-2 and RK-2). The cluster II consisted of eighteen genotypes were divided into two subclusters (IIA and IIB). MR-1, MR-2, RK-2 and CC belonging to the subcluster IIB together with *Curcuma longa voucher PH1284, Curcuma montana* and *Curcuma amada*. Interestingly, CC is closely related to *Curcuma montana* and MR-2, whereas both MR-1 and RK-2 are closely related to *Curcuma amada*.

3.2. Analysis of genetic variability by microsatellites analysis.

A total of eight SSR markers were used to evaluate of genetic variability of three samples of *CL* from Rapa Nui, which 36 different alleles were detected. The average size of PCR fragments were ranged from 50 to 1250 base pairs (*Supplementary Figure S1*). The range of allelic variants was from 2 (CMS-01) to 11 (CMS-06) with an average of 1.5 alleles per locus/amplification with a maximum

Table 2
Identification of homologous species based in ITS2 regions of *Curcuma longa* samples.

Species	Sequence identity (%)				GenBank accession number
	CC	MR-1	MR-2	RK-2	
Curcuma longa voucher PH12847	100	100	100	100	KX675001
Curcuma amada	100	100	100	100	KF304458
Curcuma haritha	98.74	98.74	98.74	98.74	KJ872076
Curcuma montana	98.34	98.34	98.34	98.34	KM983490
Curcuma ferruginea	96.71	96.71	96.71	96.71	KJ872073
Curcuma aromatica	96.71	96.71	96.71	96.71	KJ872066
Curcuma caesia	96.71	96.71	96.71	96.71	KF304479
Curcuma amarissima	96.71	96.71	96.71	96.71	KF694822
Curcuma phaeocaulis	96.71	96.71	96.71	96.71	KF694820
Curcuma yunnanensis	96.71	96.71	96.71	96.71	KF694815
Curcuma kwangsiensis	96.71	96.71	96.71	96.71	GU180361
Curcuma aeruginosa	96.69	96.69	96.69	96.69	KJ872054
Curcuma aff. prakasha	96.68	96.68	96.68	96.68	KJ803117
Curcuma zedoaria	96.68	96.68	96.68	96.68	GU180359
Curcuma flaviflora	96.28	96.28	96.28	96.28	KJ803140
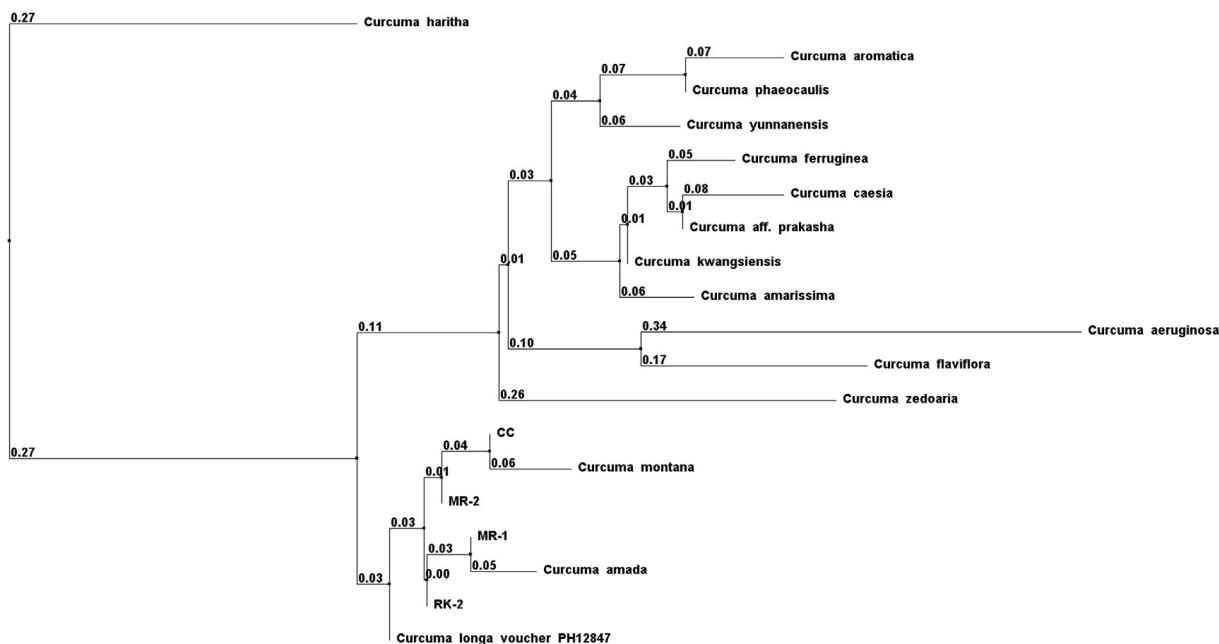
Fig. 2. Phylogenetic tree based on ITS2 sequences for *Curcuma* species using the Neighbor-Joining method. The numbers below the branches indicate the bootstrap value.

of three alleles, with a polymorphic loci percent between 0% and 50%. The results of presence or absence of bands from PCR amplifications were analyzed using the UPGMA clustering method (Fig. 3 and Supplementary Table ST2). Results showed two major clusters (I and II), group I consisted of CC sample and group II consisted of Rapa Nui samples (MR-1, MR-2 and RK-2). The cluster II consisted of three genotypes (MR-1, MR-2 and RK-2) were divided into two subclusters (IIA and IIB). The subcluster IIB, consisted of MR-1 and RK-2, exhibited the maximum similarity of 72.4%, as shown in similarity matrix (Supplementary Table ST2). Genotype MR-2 was similar to MR-1 and RK-2 with 70.8 and 42.9% similarity, whereas genotype CC was similar to RK-2, MR-1 and MR-2 with 63.9, 43.2 and 42.9% similarity, respectively.

3.3. Determination of total polyphenols, tannins and curcumin

The total content of phenolic, tannins and curcumin in the extracts from MR-1, MR-2 and RK-2 and rhizome of CC are shown in the Table 3. The results indicated that rhizomes extract of MR-1, MR-2, and RK-2 have a high content of secondary metabolites, principally polyphenols (Table 3). The Table 3 showed also that the concentration of curcumin is higher in rhizomes than leaves extracts, principally in extracts from rhizomes of MR-1 with 29.69 mg/g, being more than 6 times than the CC samples found in Peru. Compared to the other samples from Rapa Nui, MR-1 presents more than twice than those of RK-2 and almost three times more than those of MR-2.

3.4. Evaluation of antioxidant activity of hydroalcoholic extracts by DPPH and ORAC value

Despite that all the extracts present antioxidant activity (Table 4 and 5), leaves and rhizomes extract of MR-1 showed better antioxidant activity than the rest of samples, with an IC_{50} value of 0.74 µg/mL and 1.31 µg/mL, respectively. It should be noted DPPH assays showed that leaves extract of MR-1 exhibited better antioxidant activity than control sample (GA), whereas ORAC value assay showed that rhizomes extract of MR-1 exhibited better antioxidant capacity than control sample (TROLOX) with a value of 1.27 µg/mL.

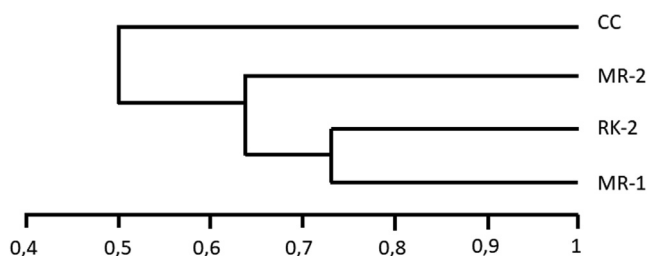**Fig. 3.** The UPGMA dendrogram of 4 *Curcuma longa* samples based on Jaccards similarity coefficients using eight SSR markers.

3.5. COX-2 inhibitor screening

Assessment of the effect of *CL* extracts on COX-2 inhibition were carried out by using BioVision® "COX-2 Inhibitor Detection Kit (Fluorometric)". Fig. 4 shows the effects at 1.5 µg/mL and 3 µg/mL of extract, using the celecoxib drug as a positive control. The rhizome extract of MR-1 have the higher degree of COX-2 inhibition than the rest of samples except for celecoxib, as shown in Figure 4 and 5 and *Supplementary Table ST3*. Furthermore, the enzyme inhibition is dependent on the concentration of the extract as well as the drug celecoxib.

Rhizome and leaves extracts of MR-1 have a greater percentage of COX-2 inhibition, followed by the rhizome extract of RK-2 (Fig. 4). Although, celecoxib has a greater inhibitory capacity than the rest of *CL* sample, the rhizome extract from MR-1 present only 36% less inhibition than celecoxib at the same concentration (3 µg/mL). It should be considered that rhizome extract of MR-1 has greater antioxidant capacity for the DPPH and ORAC assay. Furthermore, leaves extract of MR-1 has an IC_{50} value 0.74 µg/mL for DPPH and 0.73 µg/mL ORAC value. Despite ORAC value for leaves extract of MR-1 is lower than expected, it is still close to 1 and the second-best percentage of COX-2 inhibition, after the rhizome extract.

3.6. Molecular docking

Table 2 shows the predicted binding energies ($\Delta G_{binding}$) and binding sites of curcuminoid polyphenols and NAIDs with COX-2. Bisdemethoxycurcumin has a lower ΔG_{bindin} for COX-2 followed by curcumin and demethoxycurcumin, with $\Delta G_{binding}$ values −9.2, −8.8 and −8.7 Kcal/mol, respectively. Fig. 5A depicts the potential binding site and the poses of docked curcumin into COX-2. Fig. 5B shows interactions of curcumin with the COX-2 binding pocket are governed by hydrogen bonds associated with the carbonyl oxygen, which interacts with the amino of the guanidine group of Arg106 at 3.01 Å and the hydroxyl the phenolic

Table 4
The IC_{50} values of DPPH scavening and ORAC Value from *Curcuma longa* extracts (µg/mL).

| Organ	Ecotype	IC_{50} (DPPH)	ORAC Value
Leaf	MR-1	0.74 ± 0.01	0.73 ± 0.01
	MR-2	23.34 ± 0.01	0.41 ± 0.01
	RK-2	19.49 ± 0.01	0.58 ± 0.03
Rhizome	MR-1	1.31 ± 0.02	1.27 ± 0.04
	MR-2	41.97 ± 0.04	0.48 ± 0.02
	RK-2	37.29 ± 0.01	0.80 ± 0.01
	CC	19.06 ± 0.03	0.62 ± 0.02
Control	Galic Acid	0.89 ± 0.03	–
	TROLOX	–	1 ± 0.02

The values are the average ± SD of replicates performed for each experiment.

Table 3
Content of total polyphenols, tannins and curcumin in leaf and rhizome from samples of *Curcuma longa*.

Organ	Ecotype	Total polyphenols [mg/g]	Tannins [mg GAE/g]	Curcumin [mg/g]
	MR-1	3.74 ± 0.2	Under LOD	0.19 ± 0.03
Leaf	MR-2	3.14 ± 0.3	0.70 ± 0.07	1.04 ± 0.07
	RK-2	3.53 ± 0.3	Under LOD	0.22 ± 0.01
	MR-1	33.68 ± 0.4	2.57 ± 0.1	29.69 ± 0.32
Rhizome	MR-2	29.73 ± 0.1	0.89 ± 0.1	10.98 ± 0.24
	RK-2	22.74 ± 1.6	2.09 ± 0.6	14.82 ± 0.56
	CC	5.52 ± 0.02	3.93 ± 0.5	4.93 ± 0.82

The values are the average ± SD of replicates performed for each experiment. LOD: Limit of detection.

Table 5

Binding Free Energies and Binding Sites of traditional anti-inflammatory drugs and curcumin with COX-2.

Compound	$\Delta G_{binding}$ (Kcal/mol)	binding site in COX-2
curcumin	−8.8	His75, Arg106, Val335, Leu338, Ser339, Tyr341, Tyr371, Trp373, Argg499, Ile503, Phe504, Met508, Val509, Gly512, Ala513, Ser516, Leu517
demethoxycurcumin	−8.7	Arg106, Val335, Leu338, Ser339, Tyr341, Tyr371, Trp373, Phe504, Met508, Val509, Gly512, Ser516, Ala513, Leu517
bisdemethoxycurcumin	−9.2	His75, Arg106, Val335, Leu338, Ser339, Tyr341, Leu370, Trp373, Ile503, Phe504, Met508, Val509, Gly512, Ala513, Ser516, Leu517
meloxicam	−7.0	Val102, Arg106, Val335, Leu338, Ser339, Tyr341, Leu345, Leu370, Tyr371, Trp373, Met508, Val509, Glu512, Ala513, Ser516
etodolac	−8.3	Gln178, Val335, Leu338, Ser339, Tyr341, Tyr371, Trp373, Ile503, Phe504, Met508, Val509, Gly512, Ala513, Ser516
lumiracoxib	−8.9	Val102, Arg106, Val335 Leu338, Ser339, Tyr341, Leu345, Leu370, Tyr371, Trp373, Met508, Val509, Gly512, Ala513, Ser516
etoricoxib	−9.6	His75, Arg106, Val335, Leu338, Tyr341, Tyr371, Trp373, Ala502, Val509, Gly512, Ala513, Ser516, Leu517
valdecoxib	−10.2	His75, Val335, Leu338, Ser339, Tyr341, Trp373, Phe504, Val509, Gly512, Ala513
celecoxib	−10.2	His75, Val335, Leu338, Ser339, Tyr341, Tyr371, Tyr373, Arg449, Phe504, Val509, Gly512, Ala513, Ser516
rofecoxib	−10.3	His75, Val335, Leu338, Ser339, Tyr341, Trp373, Arg499, Phe504, Val509, Gly512, Ala513, Ser516

* Blue and red colored names correspond to those amino acids involved in H-bonds and hydrophobic contacts with the corresponding COX-2, respectively.
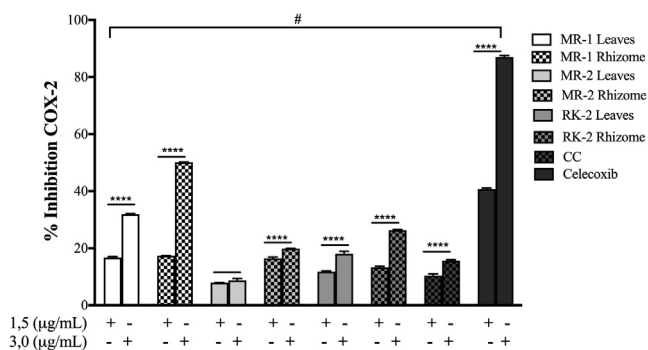
Fig. 4. COX-2 inhibitor screening.

group of Tyr341 at 3.00 Å. Additionally, the curcumin-COX-2 complex is stabilized by hydrophobic interactions with different amino acids at the binding site of COX-2, such as His75, Val335, Leu338, Ser339, Tyr371, Trp373, Argg499, Ile503, Phe504, Met508, Val509, Gly512, Ala513, Ser516, Leu517 (see Table 5).

Although three curcuminoids have a higher $\Delta G_{binding}$ for COX-2 than NAIDs corresponding to Coxib family, except for lumiracoxib, these have a lower ΔG_{bindin} than other COX-2 selective NAIDs as

etodolac and meloxicam. Additionally, Table 5 shows that all studied NAIDs and curcuminoids lies in the same binding cavity into COX-2 sharing a set of amino acids as Val335, Leu338, Val509, Glu512 and Ser516.

4. Discussions

Study reported by Zizka (1991) suggest that probably CL was introduced to Rapa Nui from Polynesia with the American colonization. However, the origin of *CL* from Rapa Nui Island is still unknown. Due to lack information and the medicinal importance for native people, we carried out phylogenetic and genetic variability analysis of three plants of *CL* collected from reservoir from Germplasm Bank from Mataveri Otai (CONAF) in Rapa Nui, using genetic marker nrDNA-ITS2 and SSR. These molecular tools are adequate to study the conservation and ecology of this plant (Arif et al., 2011). The phylogenetic analysis, based on nrDNA-ITS2 sequences, indicated that MR-1, MR-2, RK-2, CC, *Curcuma longa voucher PH1284*, *Curcuma amada* and *Curcuma montana* are part of a same subgroup. Interestingly, CC is closely related to *Curcuma montana* and MR-2, whereas both MR-1 and RK-2 are closely related to *Curcuma amada* or known as mango ginger. Additionally, the phenotypic characteristic of *C. amada* is very similar to plants grown in the Rapa Nui as MR1, for instance the color of the flowers as shown in Figure S3. Despite Curcuma is founded in South Pacific, China, Pakistan, Thailand, Malaysia, and India (Sasikumar, 2005), few reports available about its growth and distribution. On the other hand, the comparison of nrDNA ITS2 of the all studied Curcuma species, by sequences multiple alignment, revealed that there are differences in nucleotides at three different position in the DNA sequence of *Curcuma haritha*, i.e. at the alignment position 434 and 435 there were a gap, whereas at position 467 there was a "C" instead "T" (see Figure S2), which could explain that *Curcuma haritha* is distantly related to the rest of Curcuma species, including MR-1, MR-2, RK-2 and CC.

We have found two major groups, group I consisted of a sample derived from the continent (i.e. Peru) and group II consisted of Rapa Nui samples (MR-1, MR-2 and RK-2). The group II was subdivided in two subgroups, one consisted of MR-2 sample and the second one consisted RK-2 and MR-1 samples. Both groups have a similarity coefficient of 50%, whereas for both subgroups is 65% (see Fig. 3). These results could indicate that the sample MR-1, MR-2 and RK-2 come from the same lineage, being all those were collected from Germplasm Bank in Rapa Nui. However, they do not necessarily came from the same geographical location because their reservoir has received *CL* that have grown in different places on the Island in order to preserve and study them. It also is possible that MR-1 and MR-2 have been moved from same place to reservoir at different times, with MR-1 being closer to RK-2. Studies in *CL* carried out in Brazil, India and Puerto Rico using SSR, demonstrated that exist genetic variability of *CL* into the same country and the same region where were collected (Sigrist et al., 2011). This could explain the variation in the content of nutrients available in the soil, amount of rainfall, and temperature variations in Rapa Nui, could be favoring the production of certain secondary metabolites in the *CL* plants (Stevenson et al., 2015; Jungklang et al., 2017). Furthermore the genetic variability impact on the phenotype of the plant, which could explain the common trending of maintaining high genetic diversity within populations in tropical plants as reported by Hamrick and Loveless (2019).

Interestingly, our results showed a significant variation of total phenolic content in different rhizome extracts of *CL*. Indeed, a variety of *CL* rhizomes obtained in Okinawa (Japan) also showed a variation in the total phenolic content depending on the curcuma subtype (Akter et al., 2019). According to these results, the total
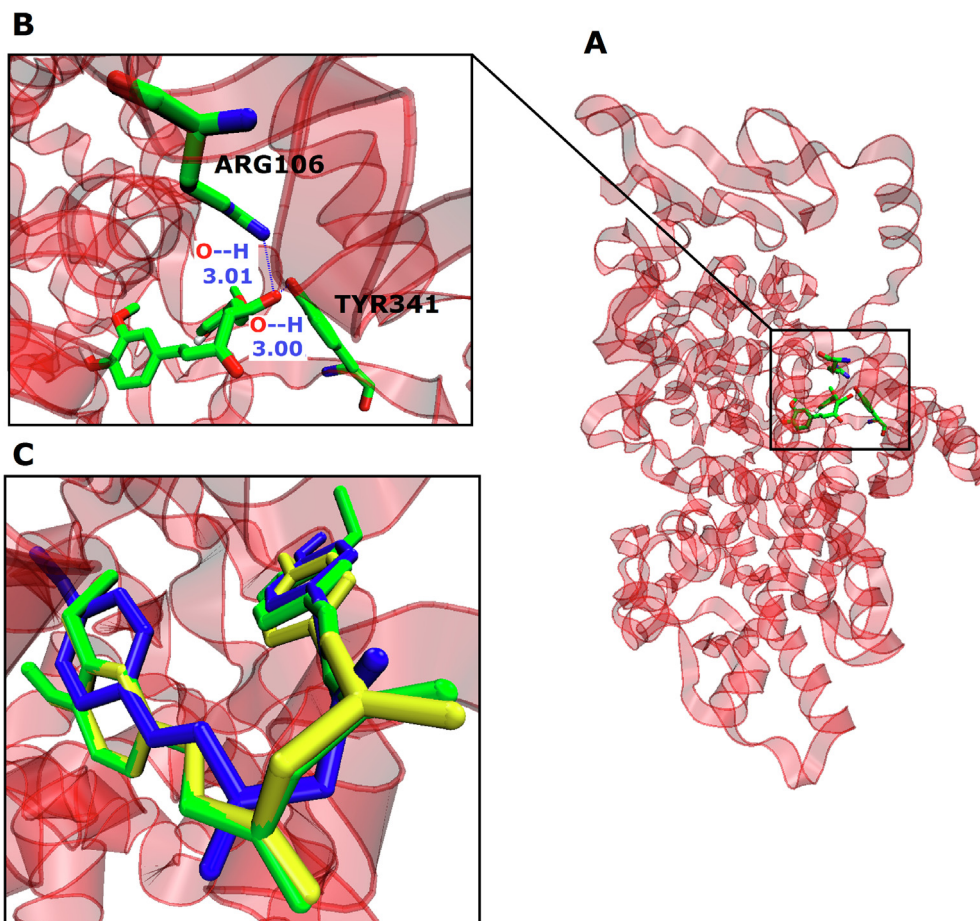
Fig. 5. Visualization of the potential binding site and docking poses of (A, B) curcumin and (C) curcuminoid polyphenols into COX-2. Curcumin, demethoxycurcumin and bisdemethoxycurcumin are in green, yellow, and blue, respectively.

phenolic content in the rhizome of *CL* from Rapa Nui is lower than those from Okinawa. However, phenolic content in these rhizomes is higher than those from Bangladesh (Tanvir et al., 2017).

Our DPPH assays and ORAC value results shows that samples from rhizomes and leaves of MR-1 exhibited better antioxidant capacity than the rest of studied samples. Although the other samples also exhibited antioxidant capacity for both tests, it is not comparable with the antioxidant capacity obtained from the standard sample (pure compound). In fact, it is important to keep in mind that other factors could play important roles in the antioxidant activities of plant materials, as structural features of the antioxidants and the complex composition of the extracts. Furthermore, polar antioxidants could remain in the aqueous phase and to be lost during the extraction process (Gálvez et al., 2005). However, our DPPH assays results are similar to the reported by Akter et al. (2019), which polar antioxidants were also found in methanolic extracts of rhizomes of *C. longa*, *C. xanthorrhiza*, *C. aromatica*, *C. amanda* and *C. zedoaria*.

Here we decided to carry out COX-2 inhibition assay for *Curcuma Longa* extracts due to that this plant has been used in traditional Rapa Nui medicine. Our COX-2 inhibition assay results showed that rhizome extracts inhibit the COX-2 activity. These findings are supported by studies reported by Mujumdar et al. (2004), which demonstrated the anti-inflammatory activity of *C. amada* rhizome on albino mice. Furthermore, these extracts could also reduce the synthesis of prostaglandin E_2 (PGE₂) by decreasing the formation of reactive oxygen species (ROS) because ROS induce the ERK activation leading to the activation of COX-2 (Hu et al.,

2017). Curcumin has been widely reported as an anti-inflammatory agent due to the ability of this compound to inhibit the activity of both COX-1 and COX-2 in the arachidonic acid metabolism (Zhang et al., 1999). Complementarily, we performed docking studies in order to understand the interactions of curcuminoids of *CL* with COX-2 at the molecular level. According to the potential curcumin binding site on COX-2, besides those identified by Elumalai et al. (2012), i.e. Arg106 and Tyr341, we showed that three curcuminoids of *CL* and selective NAIDs, as drugs belonging to Coxib family, etodolac and meloxicam, lie the same binding cavity sharing a set of amino acids, including Val335, Leu338, Val509, Glu512 and Ser516. Three curcuminoids have a lower ΔG_{bindin} than other COX-2 selective NAIDs as etodolac and meloxicam, except for Coxib family as valdecoxib, celecoxib and rofecoxib.

Various plants, used in folk and traditional medicine, have been accepted as leads for therapeutic drug development in modern medicine. Studies reported by Septembre-Malaterre et al., (2016) showed that the presence of a large number of bioactive compounds, including polyphenols, tannins and flavonoids, exhibit various biological activities. These compounds are presents in many foods and hold great potential as candidate drug due to their safety and low toxicity.

5. Conclusions

Our findings suggest that three plant of *CL* (MR-1, MR-2 and MK-2) obtained from Germplasm Bank in Rapa Nui are closely

related to other Curcuma species as *Curcuma amada* and *Curcuma montana* even though they have genetic variability. Furthermore, rhizomes of MR-1 showed better antioxidant and anti-inflammatory capacity than the rest of samples due to its high relative concentration of polyphenols and curcumin. Therefore, these results are important to take decisions about to preservation and propagation of this ecotype. Finally, it is important to note that to confirm our docking studies, would be necessary to evaluate the COX-2 inhibitory activity of other curcuminoids of *CL* as bis-demethoxycurcumin and demethoxycurcumin. Additionally, it would be very interesting to evaluate the antiproliferative activity of curcuminoids present in *CL* samples on cancer cell lines.

Acknowledgement

Appendix A

Figure S1: Pattern of eight *SSR* markers bands to *Ccurcuma longa* samples; Representative electrophoresis agarose gel showing PCR profile from MR-1, MR2, RK2 and CC using CuMiSat primer. Lane PM indicates the molecular weight marker. Figure S2: Sequence alignment of the three Rapa Nui samples and *Curcuma* species listed in Table 2; Figure S3: A). *Curcuma* plants collected from Rapa Nui; B) *Curcuma amada*; C) *Curcuma Longa* ; D) *Curcuma montana* (images obtained from: Royal Botanic Gardens Kew Seed Information Database (SID), 2020). Table ST1: Extraction percentage in grams of dry weight per 100 g from *Curcuma longa* extracts; Table ST2: Similarity matrix of 4 Curcuma longa samples calculated by the Jaccard coefficient; Table ST3: Percent of COX-2 inhibition by *Curcuma longa* extracts.

Appendix B. Supplementary material

Supplementary data to this article can be found online at https://doi.org/10.1016/j.sjbs.2020.10.062.

References

Akter, J., Hossain, M.A., Takara, K., Islam, M.Z., Hou, D.-X., 2019. Antioxidant activity of different species and varieties of turmeric (Curcuma spp): Isolation of active compounds. Comp. Biochem. Physiol. C: Toxicol. Pharmacol. 215, 9–17.

Arya, N., Prakash, O., Kumar, S., Pant, A.K., 2016. Curcumin profiling and genetic diversity of different accessions of Curcuma longa L. Asian Pacific J. Trop. Dis. 6, 70–74. https://doi.org/10.1016/S2222-1808(15)60987-2.

Arif, I.A., Khan, H.A., Bahkali, A.H., Al Homaidan, A.A., Al Farhan, A.H., Al Sadoon, M., Shobrak, M., 2011. DNA marker technology for wildlife conservation. Saudi J. Biological Sci. 18, 219–225.

Berman, H.M., Westbrook, J., Feng, Z., Gilliland, G., Bhat, T.N., Weissig, H., Shindyalov, I.N., Bourne, P.E., 2000. The Protein Data Bank. Nucleic Acids Res. 28, 235–242. https://doi.org/10.1093/nar/28.1.235.

Chattopadhyay, N.R., 2017. Genetic Variation and Phylogenetic Relationship Among the Two Different Stocks of Catla (Catla catla) in the Indian State of Orissa Based on RAPD Profiles, Induced Fish Breeding Academic Press, pp. 267 -301. https://doi.org/10.1016/b978-0-12-801774-6.00010-9.

Chen, Y., Jobanputra, P., Barton, P., Bryan, S., Harris, G., Taylor, R.S., 2008. Cyclooxygenase-2 selective non-steroidal anti-inflammatory drugs (etodolac, meloxicam, celecoxib, rofecoxib, etoricoxib, valdecoxib and lumiracoxib) for osteoarthritis and rheumatoid arthritis: a systematic review and economic evaluation. Health Technol. Assess. (Rockv). 12, 1–297. https://doi.org/10.3310/hta12110.

Chen, S., Yao, H., Han, J., Liu, C., Song, J., Shi, L., Zhu, Y., Ma, X., Gao, T., Pang, X., Luo, K., Li, Y., Li, X., Jia, X., Lin, Y., Leon, C., 2010. Validation of the ITS2 region as a novel DNA barcode for identifying medicinal plant species. PLoS One. 5, 1–8. https://doi.org/10.1371/journal.pone.0008613.

Brand-Williams, W., Cuvelier, M.E., Berset, C., 1995. Use of a free radical method to evaluate antioxidant activity. LWT - Food Science and Technology 28, 25–30.

Dubios. A., Lenne. P., Nahoe. E., Rauch. M., 2013. Plantas de RaPa nui. Guía Ilustrada de la Flora de Interés Ecológico y Patrimonial. First ed. Umanga mo te Natura, CONAF, ONF International, Santiago, pp. 55.

Dávalos, A., Gómez-Cordovés, C., Bartolomé, B., 2004. Extending Applicability of the Oxygen Radical Absorbance Capacity (ORAC−Fluorescein) Assay. J. Agric. Food Chem. 52, 48–54.

Duvoix, A., Blasius, R., Delhalle, S., Schnekenburger, M., Morceau, F., Henry, E., Dicato, M., Diederich, M., 2005. Chemopreventive and therapeutic effects of curcumin. Cancer Lett. 223, 181–190.

Efthymiopoulos, I., Hellier, P., Ladommatos, N., Kay, A., Mills-Lamptey, B., 2019. Effect of Solvent Extraction Parameters on the Recovery of Oil From Spent Coffee Grounds for Biofuel Production. Waste Biomass Valor 10, 253–264.

Elumalai, M., Muthaiah, R., Ali, M.A., 2012. Identification of Curcumin Targets in Neuroinflammatory Pathways: Molecular Docking Scores with GSK-3β, P38 MAPK, COX, ICE and TACE Enzymes. Acta Pol. Pharm. 69, 237–245.

Feng, S., Jiang, M., Shi, Y., Jiao, K., Shen, C., Lu, J., 2016. Application of the Ribosomal DNA ITS2 Region of Physalis (Solanaceae): DNA Barcoding and Phylogenetic Study. Front. Plant Sci. 7, 1–11. https://doi.org/10.3389/fpls.2016.01047.

Gálvez, M., Martín-Cordero, C., Houghton, P.J., Ayuso, M.J., 2005. Antioxidant Activity of Methanol Extracts Obtained from Plantago Species. J. Agric. Food Chem. 53, 1927–1933.

Garcia-Vallve, S., Palau, J., Romeu, A., 1999. Horizontal gene transfer in glycosyl hydrolases inferred from codon usage in Escherichia coli and Bacillus subtilis. Mol. Biol. Evol. 16, 1125–1134.

Hamrick, J.L., Loveless, M., 2019. The Genetic Structure of Tropical Tree Populations: Associations with Reproductive Biology, in: The Evolutionary Ecology of Plants. pp. 129–146. https://doi.org/10.1201/9780429310720-8.

Guzmán, L., Villalón, K., Marchant, M.J., Tarnok, M.E., Cárdenas, P., Aquea, G., Acevedo, W., Padilla, L., Bernal, G., Molinari, A., Corvalán, A., 2020. In vitro evaluation and molecular docking of QS-21 and quillaic acid from *Quillaja saponaria* Molina as gastric cancer agents. Sci. Rep. 10. https://doi.org/10.1038/s41598-020-67442-3.

Hatcher, H., Planalp, R., Cho, J., Torti, F.M., Torti, S.V., 2008. Curcumin: From ancient medicine to current clinical trials. Cell. Mol. Life Sci. 65, 1631–1652.

Hayakawa, H., Minaniya, Y., Ito, K., Yamamoto, Y., Fukuda, T., 2011. Difference of Curcumin Content in *Curcuma longa* L. (Zingiberaceae) Caused by Hybridization with Other Curcuma Species. AJPS. 02, 111–119.

Hazra, K., Kumar, R., Kumar Sarkar, B., Chowdary, Y.A., Devgan, M., Ramaiah, M., Educational, R.P., 2015. Uv-Visible Spectrophotometric Estimation of Curcumin in Nano-Formulation. Int. J. Pharmacogn. 2, 127–130 https://doi.org/10.13040/IJPSR.0975-8232.

Hu, Y.-P., Peng, Y.-B., Zhang, Y.-F., Wang, Y., Yu, W.-R., Yao, M., Fu, X.-J., 2017. Reactive Oxygen Species Mediated Prostaglandin E 2 Contributes to Acute Response of Epithelial Injury. Oxid. Med. Cell. Longevity 2017, 1–8.

Humphrey, W., Dalke, A., Schulten, K., 1996. VMD: Visual molecular dynamics. J. Mol. Graph. 14, 33–38.

Jungklang, J., Saengnil, K., Uthaibutra, J., 2017. Effects of water-deficit stress and paclobutrazol on growth, relative water content, electrolyte leakage, proline content and some antioxidant changes in Curcuma alismatifolia Gagnep. cv. Chiang Mai Pink. Saudi J. Biological Sci. 24, 1505–1512.

Prasad, S., Aggarwal, B.B., 2011. Turmeric, the Golden Spice: From Traditional Medicine to Modern Medicine., in: Benzie, I.F.F., Wachtel-Galor, S. (Eds.), Herbal Medicine: Biomolecular and Clinical Aspects. Boca Raton (FL).

Kocaadam, B., Şanlier, N., 2017. Curcumin, an active component of turmeric (*Curcuma longa*), and its effects on health. Crit. Rev. Food Sci. Nutr. 57, 2889–2895.

Mujumdar, A.M., Naik, D.G., Misar, A.V., Puntambekar, H.M., Dandge, C.N., 2004. CNS Depressant and Analgesic Activity of a Fraction Isolated from an Ethanol Extract of *Curcuma amada* Rhizomes. Arch. Physiol. Biochem. 42, 542–546.

Ou, B., Hampsch-Woodill, M., Prior, R.L., 2001. Development and Validation of an Improved Oxygen Radical Absorbance Capacity Assay Using Fluorescein as the Fluorescent Probe. J. Agric. Food Chem. 49, 4619–4626.

Ricco, R.A., Agudelo, I.J., Wagner, M.L., 2015. Métodos empleados en el análisis de los polifenoles en un laboratorio de baja complejidad. Lilloa 52, 161–174. 10.30550/j.lil.

Sasikumar, B., 2005. Genetic resources of Curcuma : diversity, characterization and utilization. Plant Genet. Resour. 3, 230–251. https://doi.org/10.1079/pgr200574.

Septembre-Malaterre, A., Stanislas, G., Douraguia, E., Gonthier, M.-P., 2016. Evaluation of nutritional and antioxidant properties of the tropical fruits banana, litchi, mango, papaya, passion fruit and pineapple cultivated in Réunion French Island. Food Chem. 212, 225–233.

Sigrist, M.S., Pinheiro, J.B., Azevedo-Filho, J.A., Colombo, C.A., Bajay, M.M., Lima, P.F., Camilo, F.R., Sandhu, S., Souza, A.P., Zucchi, M.I., 2010. Development and characterization of microsatellite markers for turmeric (*Curcuma longa*). Plant Breed. 129, 570–573. https://doi.org/10.1111/j.1439-0523.2009.01720.x.

Sigrist, M.S., Pinheiro, J.B., Azevedo, J. de, Zucchi, M.I., 2011. Genetic diversity of turmeric germplasm (Curcuma longa; Zingiberaceae) identified by microsatellite markers. Genet. Mol. Res. 10, 419–28. https://doi.org/10.4238/vol10-1gmr1047.

Siju, S., Dhanya, K., Syamkumar, S., Sasikumar, B., Sheeja, T.E., Bhat, A.I., Parthasarathy, V.A., 2010. Development, Characterization and Cross Species Amplification of Polymorphic Microsatellite Markers from Expressed Sequence Tags of Turmeric (*Curcuma longa* L.). Mol. Biotechnol. 44, 140–147.

Stevenson, C.M., Puleston, C.O., Vitousek, P.M., Chadwick, O.A., Haoa, S., Ladefoged, T.N., 2015. Variation in Rapa Nui (Easter Island) land use indicates production and population peaks prior to European contact. PNAS 112, 1025–1030.

Strimpakos, A.S., Sharma, R.A., 2008. Curcumin: Preventive and Therapeutic Properties in Laboratory Studies and Clinical. Antioxid. Redox Signal. 10, 511–546. https://doi.org/10.1089/ars.2007.1769.

Tanvir, E.M., Hossen, M.S., Hossain, M.F., Afroz, R., Gan, S.H., Khalil, M.I., Karim, N., 2017. Antioxidant Properties of Popular Turmeric (*Curcuma longa*) Varieties from Bangladesh. J. Food Qual. 2017, 1–8.

Thompson, J.D., Higgins, D.G., Gibson, T.J., 1994. CLUSTAL W: improving the sensitivity of progressive multiple sequence alignment through sequence weighting, position-specific gap penalties and weight matrix choice. Nucl Acids Res. 22, 4673–4680.

Tomeh, M.A., Hadianamrei, R., Zhao, X., 2019. A Review of Curcumin and Its Derivatives as Anticancer Agents. Mol. Sci. 20, 1–26. https://doi.org/10.3390/ijms20051033.

Tóth, G., Gáspári, Z., Jurka, J., 2000. Microsatellites in different eukaryotic genomes: survey and analysis. Genome Res. 10, 967–981. https://doi.org/10.1101/gr.10.7.967.

Waterhouse, A.M., Procter, J.B., Martin, D.M.A., Clamp, M., Barton, G.J., 2009. Jalview Version 2–a multiple sequence alignment editor and analysis workbench. Bioinformatics 25, 1189–1191.

Xu, L., Stevens, J., Hilton, M.B., Seaman, S., Conrads, T.P., Veenstra, T.D., Logsdon, D., Morris, H., Swing, D.A., Patel, N.L., Kalen, J., Haines, D.C., Zudaire, E., St Croix, B., 2014. COX-2 inhibition potentiates antiangiogenic cancer therapy and prevents metastasis in preclinical models. Sci. Transl. Med. 6, 1–12. https://doi.org/10.1126/scitranslmed.3008455.

Zhang, F., Altorki, N.K., Mestre, J.R., Subbaramaiah, K., Dannenberg, A.J., 1999. Curcumin inhibits cyclooxygenase-2 transcription in bile acid- and phorbol ester-treated human gastrointestinal epithelial cells. Carcinogenesis 20, 445–451. https://doi.org/10.1093/carcin/20.3.445.

Xiang, Z., Wang, X.-Q., Cai, X.-J., Zeng, S.u., 2011. Metabolomics Study on Quality Control and Discrimination of Three Curcuma Species based on Gas Chromatograph-Mass Spectrometry: Metabolomics Quality Control and Discrimination of Curcuma. Phytochem. Anal. 22, 411–418.

Zizka, G., 1991. Flowering Plants of Easter Island. Frankfurt, Stadt Frankfurt Am Main, p. 84.